



# PixR, a Novel Activator of Conjugative Transfer of IncX4 Resistance Plasmids, Mitigates the Fitness Cost of *mcr-1* Carriage in *Escherichia coli*

Lingxian Yi,<sup>a,b</sup>  Romain Durand,<sup>c\*</sup> Frédéric Grenier,<sup>c</sup> Jun Yang,<sup>a,b</sup> Kaiyang Yu,<sup>a,b</sup>  Vincent Burrus,<sup>c</sup>  Jian-Hua Liu<sup>a,b</sup>

<sup>a</sup>College of Veterinary Medicine, National Risk Assessment Laboratory for Antimicrobial Resistance of Microorganisms in Animals, Guangdong Provincial Key Laboratory of Veterinary Pharmaceutics Development and Safety Evaluation, South China Agricultural University, Guangzhou, China

<sup>b</sup>Guangdong Laboratory for Lingnan Modern Agriculture, Guangzhou, China

<sup>c</sup>Département de biologie, Université de Sherbrooke, Sherbrooke, Québec, Canada

Lingxian Yi and Romain Durand contributed equally to this work.

**ABSTRACT** The emergence of the plasmid-borne colistin resistance gene *mcr-1* threatens public health. IncX4-type plasmids are one of the most epidemiologically successful vehicles for spreading *mcr-1* worldwide. Since MCR-1 is known for imposing a fitness cost to its host bacterium, the successful spread of *mcr-1*-bearing plasmids might be linked to high conjugation frequency, which would enhance the maintenance of the plasmid in the host without antibiotic selection. However, the mechanism of IncX4 plasmid conjugation remains unclear. In this study, we used high-density transposon mutagenesis to identify factors required for IncX4 plasmid transfer. Eighteen essential transfer genes were identified, including five with annotations unrelated to conjugation. Cappable-seq, transcriptome sequencing (RNA-seq), electrophoretic mobility shift assay, and  $\beta$ -galactosidase assay confirmed that a novel transcriptional regulator gene, *pixR*, directly regulates the transfer of IncX4 plasmids by binding the promoter of 13 essential transfer genes to increase their transcription. PixR is not active under nonmating conditions, while the expression of the *pixR*, *pilX3-4*, and *pilX11* genes increased 3- to 6-fold upon contact with recipient *Escherichia coli* C600. Plasmid invasion and coculture competition assays revealed the essentiality of *pixR* for spreading and persistence of *mcr-1*-bearing IncX4 plasmids in bacterial populations. Effective conjugation is crucial for alleviating the fitness cost exerted by *mcr-1* carriage. The existence of the IncX4-specific *pixR* gene increases plasmid transmissibility while promoting the invasion and persistence of *mcr-1*-bearing plasmids in bacterial populations, which helps explain their global prevalence.

**IMPORTANCE** The spread of clinically relevant antibiotic resistance genes is often linked to the dissemination of epidemic plasmids. However, the underlying molecular mechanisms contributing to the successful spread of epidemic plasmids remain unclear. In this report, we shine a light on the transfer activation of IncX4 plasmids. We show how conjugation promotes the invasion and persistence of IncX4 plasmids within a bacterial population. The dissection of the regulatory network of conjugation helps explain the rapid spread of epidemic plasmids in nature. It also reveals potential targets for the development of conjugation inhibitors.

**KEYWORDS** IncX4, conjugation, fitness, *mcr-1*, plasmids

Antimicrobial resistance is a developing global health threat. The emergence and extensive spread of multidrug-resistant (MDR) bacterial pathogens, especially Gram-negative bacteria, have made many infections, such as pneumonia, blood poisoning, and foodborne diseases, harder to treat due to less effective antibiotics, thus increasing morbidity, mortality, and medical costs (1). Plasmids play a significant role in

**Editor** Robert A. Bonomo, Louis Stokes Veterans Affairs Medical Center

**Copyright** © 2022 Yi et al. This is an open-access article distributed under the terms of the [Creative Commons Attribution 4.0 International license](https://creativecommons.org/licenses/by/4.0/).

Address correspondence to Vincent Burrus, [vincent.burrus@usherbrooke.ca](mailto:vincent.burrus@usherbrooke.ca), or Jian-Hua Liu, [jhliu@scau.edu.cn](mailto:jhliu@scau.edu.cn).

\*Present address: Romain Durand, Institut de Biologie Intégrative et des Systèmes, Université Laval, Québec, Canada.

The authors declare no conflict of interest.

**Received** 26 October 2021

**Accepted** 19 November 2021

**Published** 4 January 2022

the evolution of MDR organisms (2). Plasmid-borne antibiotic resistance genes can efficiently spread within bacterial communities across diverse species, driving antibiotic resistance evolution and threatening our ability to treat bacterial infections by restricting treatment options (3). The rise of carbapenem-resistant *Enterobacteriaceae* (CRE) and extended-spectrum beta-lactamase (ESBL)-producing *Enterobacteriaceae* is the most alarming example. The World Health Organization (WHO) listed these microorganisms as critical pathogens for which the development of new treatments is a high priority due to the global spread of plasmid-borne carbapenem resistance and ESBL genes (4). Colistin (CI) is one of a few effective options to treat infections caused by CRE. However, the emergence and dissemination of the plasmid-borne colistin resistance gene *mcr-1* limit the efficacy of colistin, causing worldwide concern (5).

Previous work revealed that IncX4 plasmids are the second most prevalent epidemic vectors carrying *mcr-1* after IncI2 plasmids (6–8). As of October 2021, IncX4 plasmids carrying *mcr-1* have been identified in *Escherichia coli*, *Salmonella enterica* (serovars Typhimurium, Paratyphi B, Java, Anatum, and Schwartzengrund), *Klebsiella pneumoniae*, and *Enterobacter cloacae* isolated from humans, food products, livestock, wildlife, and environmental samples across more than 41 countries and regions (see Fig. S1A and Table S1 in the supplemental material) (9–12). Besides *mcr-1*, IncX4 plasmids also disseminate the 23S rRNA methyltransferase gene *ctr* and the extended-spectrum  $\beta$ -lactamase and carbapenemase genes *bla*<sub>TEM</sub>, *bla*<sub>CTX-M</sub>, *bla*<sub>OXA</sub>, and *bla*<sub>NDM</sub> (13, 14).

Bacterial immunity systems, such as CRISPR-Cas or restriction-modification (RM) systems, can restrict the entry and establishment of antibiotic resistance plasmids, recognized as exogenous DNA. These plasmids also inflict a fitness cost on the host, leading to their loss in the absence of selective pressure (15–17). Paradoxically, in natural settings, epidemic antibiotic resistance plasmids can persist in bacterial populations over the long term without antibiotic selection. The latest theory explaining this “plasmid-paradox” examines three main features: the rate of plasmid loss during replication, the rate of plasmid acquisition, and the plasmid fitness adaptation to the host (2, 18, 19). Conjugation plays an essential role in the persistence of a plasmid in a bacterial population (20–22). Previous reports have shown that IncX4 plasmids transfer at a high frequency,  $\sim 10^{-2}$  to  $10^{-4}$  (23, 24). Although the rapid transmission of *mcr-1*-bearing IncX4 plasmids sparked intense concerns, most of the research conducted to date has focused only on their epidemiology. Hence, the mechanisms that have enabled IncX4 plasmids to become successful vectors for the global spread of *mcr-1*, adapt to hosts such as *E. coli*, and maintain antibiotic resistance genes in natural bacterial communities are unclear. The conjugative transfer function of genes *taxB-pilX-taxCA* of IncX4 plasmids was predicted based on sequence similarity with the IncX family reference plasmid R6K. R6K encodes a P-type (*virB*) type IV secretion system (T4SS), PilX1-PilX11, involved in pilus synthesis and assembly. It also encodes the relaxase TaxC, the auxiliary factor TaxA, and the coupling protein TaxB, which are involved in DNA processing during conjugation (GenBank accession no. [AJ006342](https://www.ncbi.nlm.nih.gov/nuccore/AJ006342)) (25). However, the genes carried by IncX4 plasmids share limited sequence identity (<60%) with those of R6K (24). Hence, the determinants of IncX4 plasmid transfer remain largely unknown, and the regulation of their transfer is poorly understood. Plasmid transfer inflicts a fitness cost due to the high ATP demand to synthesize the mating channel and energize the translocation of plasmid DNA into the recipient cell (26). To minimize this burden, the expression of the conjugative transfer genes is usually tightly controlled by plasmid- and host-encoded factors (17). The factors involved in the regulation of IncHI, IncA, IncC, IncP, and F-like plasmids are now well characterized (27–30). In contrast, little is known about the control of IncX conjugation.

In this study, we used a systematic approach to identify the genes required for IncX4 plasmid transfer and characterized an IncX4-specific transcriptional activator, PixR, that controls plasmid conjugation. Our results indicate that efficient conjugation alleviates the fitness cost of low-copy *mcr-1* carriage and promotes the persistence and

invasion of *mcr-1*-bearing plasmids within a bacterial population, which helps explain the successful dissemination of *mcr-1*-bearing plasmids in nature.

## RESULTS

**Identification of the genes involved in the transfer of IncX4 plasmids.** pHNSHP23 is an *mcr-1*-bearing IncX4 plasmid found in an *E. coli* strain of pig origin (7). The nucleotide sequence of pHNSHP23 was compared using BLASTN to a total of 271 IncX4 plasmids from diverse geographical origins, found in the GenBank database. We found that the IncX4 plasmids have a common structure with the predicted conjugative transfer locus sharing an average of 96% identity over 15 kb. A total of 178 out of the 271 *mcr-1*-positive IncX4 plasmid sequences are highly similar to pHNSHP23 (Fig. S2). Hence, we used pHNSHP23 as the prototype IncX4 plasmid for identifying all the transfer genes of IncX4 plasmids. High-density transposon mutagenesis (HDTM) was used to construct Tn5 insertion mutant libraries of pHNSHP23 in *E. coli* BW25113. In the initial mutant library (input library), Tn5 insertions were distributed evenly across pHNSHP23, except in the gene *pir* required for IncX4 replication, the recently identified antitoxin-encoding gene *tsxB* involved in IncX4 plasmid maintenance, and the selection marker *mcr-1* (Fig. 1). The input library was then used in a mating assay on agar using *E. coli* MG1655 as the recipient strain. The resulting transconjugants were used for a second transfer on agar (output library). Mapping of the Tn5 insertions in the output library revealed 18 genes identified as essential factors for conjugation, including the 10 *pilX* genes, the relaxase-encoding gene *taxC*, and DNA processing genes *taxA* and *taxB* (Fig. 1 and 2A). In addition, five genes previously regarded as unrelated to conjugation seemed potentially essential for IncX4 plasmid transfer, including the recently reported toxin-encoding gene *tsxA* and four genes of unknown function: *cds4*, *cds9*, *cds10*, and *cds16* (Fig. 1 and 2A). To confirm the impact of these four genes on conjugation, we constructed individual null mutants and tested their transfer by conjugation in broth. We observed the abolition of pHNSHP23 $\Delta$ *cds9* transfer. Compared to that of wild-type (WT) pHNSHP23, the transfer frequency of the  $\Delta$ *cds4* and  $\Delta$ *cds16* mutants was reduced ~4-fold, which was not statistically significant, whereas the transfer frequency of pHNSHP23 $\Delta$ *cds10* was reduced ~100-fold (Fig. 2B). Expression of *pixR* from the arabinose-inducible promoter  $P_{BAD}$  ( $pBAD$ -*pixR*) or its native promoter ( $pHSG575$ -*cds10*) restored the conjugation phenotype of  $\Delta$ *cds10* beyond the wild-type level (Fig. 2B). However, *cds9* ectopically expressed from either  $pBAD$ -*cds9* or  $pHSG575$ -*cds9* failed to complement the transfer of the  $\Delta$ *cds9* mutant, indicating that the transfer deficiency of  $\Delta$ *cds9* probably results from a polar effect on the downstream genes. Hence, we focused on the hypothetical gene *cds10* because its deletion inhibited conjugation, whereas complementation increased transfer compared to that of the WT. pHNSHP23 and its  $\Delta$ *cds10* mutant were introduced into *E. coli* GDE8P261, a strain isolated from swine, to test whether the effect of *pixR* was strain specific. Conjugation phenotypes similar to those obtained with BW25113 confirmed that *pixR* acts in a strain-independent manner (Fig. 2B).

**PixR is a key activator controlling IncX4 plasmid transfer.** The hypothetical gene *cds10* is a conserved feature of IncX4 plasmids, missing in other IncX subgroups. Hence, we hypothesized that *cds10* is an IncX4-specific conjugation factor. Based on the evidence presented below suggesting that *cds10* encodes a regulator of the expression of the *pilX* operon, we renamed it *pixR* (*pilX* regulator). The gene *pixR* is located directly downstream of *taxC* and upstream of the pilus assembly-related genes (Fig. 1). *pixR* encodes a 10.8-kDa hypothetical protein of 97 amino acid residues with a predicted HTH DNA-binding domain (Pfam PF08281). The predicted structure of PixR obtained using phyre2 (<http://www.sbg.bio.ic.ac.uk/phyre2/>) suggests that PixR<sub>3-79</sub> folds like the C-terminal domain of LuxR-type regulators despite low primary sequence identity (13 to ~29%) (Fig. 2C). LuxR proteins act as pheromone receptors and transcriptional regulators, affecting bacterial survival and propagation, virulence, and biofilm formation (31). The C-terminal domain of LuxR-type proteins typically binds specific DNA sites upon binding of an autoinducer (AI) to its N-terminal domain (31). However, PixR seems to lack the ligand-binding domain.

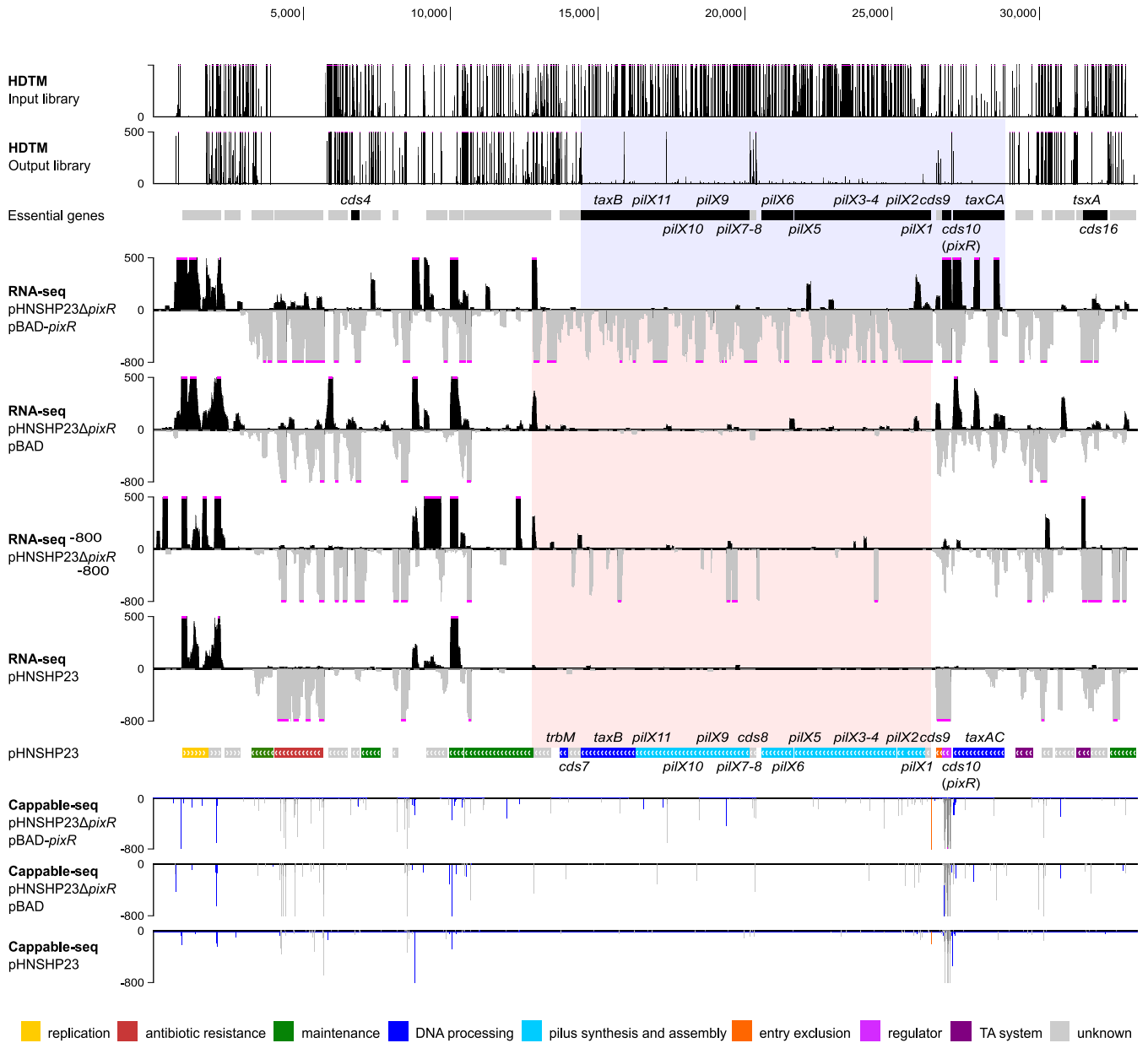


**FIG 1** In-depth analysis of the PixR regulon. The first two tracks represent the Tn5 insertions sites in the mutant libraries before and after two consecutive matings, respectively. Essential genes appear in black in the “essential genes” track. The region highlighted in blue encompasses the ones belonging to the transfer region. The following four tracks represent the RNA-seq read densities of *E. coli* BW25113/pHNSHP23 and BW25113/pHNSHP23Δ*pixR* carrying pBAD or pBAD-*pixR* with 0.2% arabinose induction. For each of these tracks, densities with a positive value correspond to the positive DNA strand, whereas densities with a negative value correspond to the negative DNA strand. The region highlighted in red encompasses all genes in the transfer region showing a drastic change in expression. The eighth track is the genetic map of pHNSHP23. Genes are color coded according to their predicted function as indicated in the key. The last three tracks represent the Cappable-seq results. Strains are detailed on the left. Blue and gray bars indicate the Cappable-seq density on the positive and negative DNA strands, respectively. The orange bar indicates the TSS of the *pilX* operon. For all tracks, pink dots at the summit of peaks indicate that the signal is beyond the fixed y axis maximal or minimal value.

To further demonstrate the role of *pixR* in conjugation, we tested and compared the transfer efficiency of pHNSHP23 and its Δ*pixR* mutant in mating assays conducted both on agar plates and in broth. pHNSHP23 transferred at much higher rates on agar than in broth ( $2.19 \times 10^{-2}$  versus  $1.73 \times 10^{-5}$ , respectively). pHNSHP23Δ*pixR* exhibited a 2-log reduction of transfer frequency in broth ( $1.73 \times 10^{-5}$  versus  $1.25 \times 10^{-7}$ ) and an ~5-log reduction on agar ( $2.19 \times 10^{-2}$  versus  $1.18 \times 10^{-7}$ ) (Fig. 2D), suggesting that PixR acts as a key conjugation regulator both on a solid surface and in liquid. Transfer of the Δ*pixR* mutant was restored and even enhanced above the wild-type level



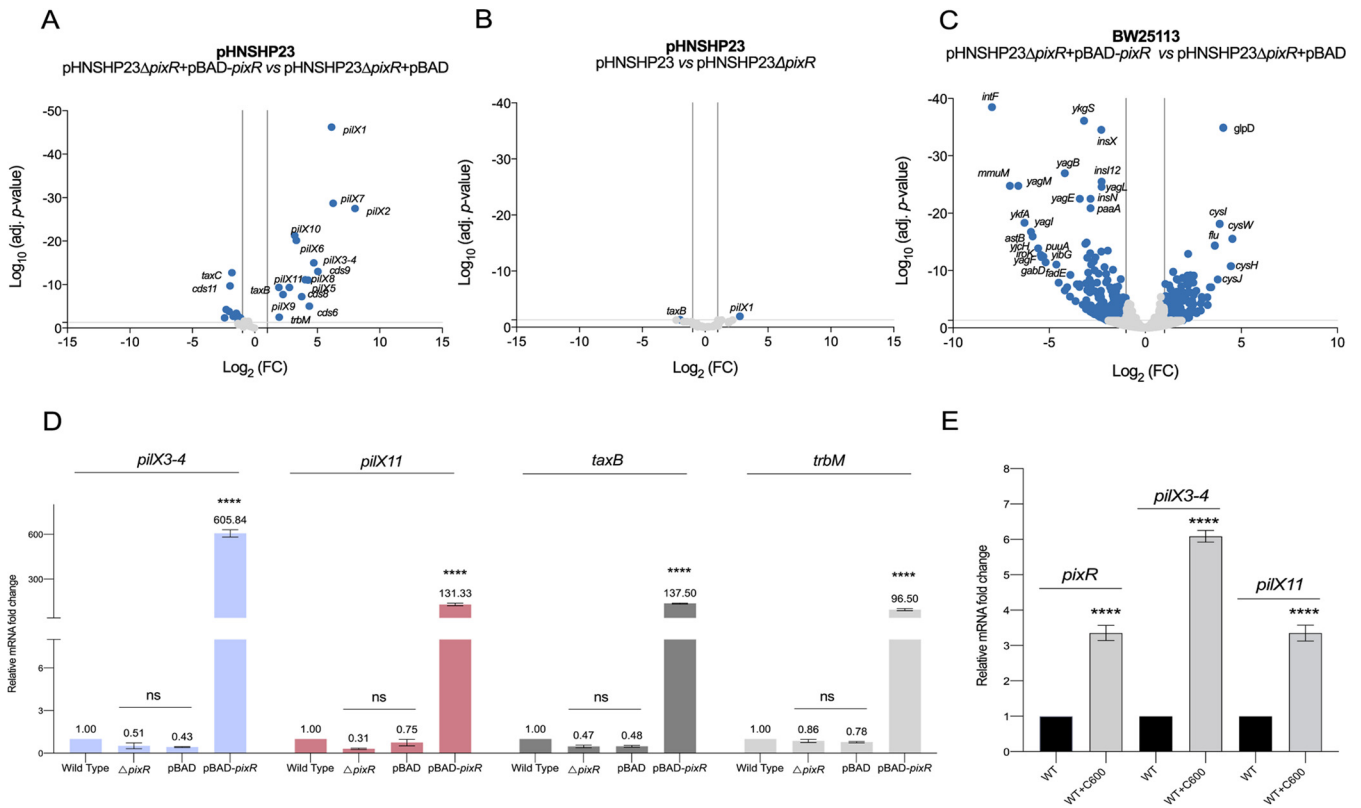


**FIG 3** PixR regulon. (A and B) Differential expression analyses of pHNSHP23 genes upon *pixR* overexpression or deletion. (C) Differential expression analysis of BW25113 genes upon *pixR* overexpression. The x and y axes represent the log<sub>2</sub> fold change and the adjusted P value, respectively. The vertical lines represent a 2-fold change in expression. Genes were considered differentially expressed (and therefore were marked with blue dots) when they displayed a fold change of more than 2 as well as an adjusted P value of more than 0.05, indicated by the gray horizontal line. (D) Effect of *pixR* deletion on the mRNA level of *pilX3-4*, *pilX11*, *taxB*, and *trbM*. The bars represent the means and standard deviations from biological triplicates. Four distinct one-way ANOVAs with Tukey’s multiple-comparison test were performed to compare the relative mRNA levels of a given gene or operon under different conditions. Statistical significance is indicated as follows: \*\*\*\*, P < 0.0001. (E) mRNA levels of *pixR*, *pilX3-4*, and *pilX11* with and without C600 contact. The bars represent the means and standard deviations from biological triplicates. Bars were compared using unpaired t test.

upon overexpression of *pixR* from the arabinose-inducible promoter *P*<sub>BAD</sub> (Fig. 2D). This observation indicates that *pixR* acts as a potent enhancer of the transmissibility of IncX4 plasmids.

**Overexpression of *pixR* upregulates the transcription of the transfer genes.** To explore how *pixR* regulates the transfer of IncX4 plasmids, we performed a transcriptome sequencing (RNA-seq) experiment to determine the transcriptional profile of pHNSHP23 and its  $\Delta$ *pixR* mutant upon overexpression of *pixR* in *E. coli* BW25113. We found that the expression of 15 genes within an ~15-kb region increased considerably upon overexpression of *pixR* (Fig. 1). Differential expression analyses confirmed that overexpression of *pixR* resulted in a 4.7- to 250-fold increase of expression of the *pilX* genes (Fig. 3A). Expression of *taxB* and *trbM* also increased 4.8-fold, whereas expression of three genes of unknown function (*cds6*, *cds8*, and *cds9*) increased 13-fold (Fig. 3A). These observations suggest that PixR activates the transcription of a set of genes involved in IncX4 plasmid transfer. However, the expression levels were virtually identical between pHNSHP23 and its  $\Delta$ *pixR* mutant (Fig. 3B). Perhaps *pixR* is not expressed under the laboratory conditions of RNA extraction in pure culture without a recipient strain. Alternatively, the translation product of *pixR* is inactive or sequestered, preventing activation of transfer functions.

Five hundred eight chromosomal genes were differentially expressed upon *pixR* overexpression (Fig. 3C). A pathway enrichment analysis showed that two pathways are significantly upregulated upon overexpression of *pixR*: ribosome (eco03010) and aminoacyl-tRNA biosynthesis (eco00970). Two pathways are also significantly downregulated: phenylalanine

metabolism (eco00360) and flagellar assembly (eco02040) (Table S4). Surprisingly, several of the most downregulated chromosomal genes belong to the cryptic prophage CP4-6 (Table S5). The expression changes in the host chromosomal genes are likely indirect and may be related to the burden caused by the conjugative transfer.

We performed reverse transcription followed by quantitative PCR (RT-qPCR) to confirm the RNA-seq data. Consistent with the results described above, the mRNA levels of *pilX3-4*, *pilX11*, *taxB*, and *trbM* increased more than 96-fold upon overexpression of *pixR* (Fig. 3D). In contrast, a change in expression of less than 3-fold could be observed for the same set of genes when comparing pHNSHP23 with its  $\Delta$ *pixR* mutant (Fig. 3D).

To confirm whether contact with the recipient cell influences the expression of *pixR*, we measured the relative expression of *pixR*, *pilX3-4*, and *pilX11* with and without initial coinoculation with recipient strain *E. coli* C600. The mRNA levels of *pixR*, *pilX3-4*, and *pilX11* increased 3- to 6-fold after contact with C600 (Fig. 3E).

**PixR directly activates the *pilX* operon.** The presence of a predicted HTH DNA-binding domain in PixR suggests that PixR regulates the transcription of the transfer genes by binding to the promoter region upstream of *pilX1*. We used Cappable-seq to identify the transcriptional start sites (TSS) and compared the resulting profiles with and without *pixR* overexpression. A single peak located at 26,338 bp was observed exactly 42 bp upstream of *cds9* when *pixR* was overexpressed but not with the empty vector control, indicating that the RNA polymerase complex is recruited at this locus upon overexpression of *pixR*. No other peak was reliably detected downstream in the transfer region, suggesting that the genes *cds9*, *pilX1-6*, *cds8*, *pilX7-11*, *taxB*, and *trbM* are all part of a single long operon, here referred to as the *pilX* operon (Fig. 1). This organization is reminiscent of the *virB* genes of the archetypical P-type T4SS encoded by *Agrobacterium tumefaciens*, also arranged as a single operon (25, 32). However, the *pilX* operon of pHNSHP23 also includes *trbM* and *taxB* (Fig. 4A). To further confirm this, a reverse transcription experiment was performed using a primer located at the 3' end of *trbM* and total RNA extracted from *E. coli* BW25113 bearing pHNSHP23. A PCR amplification using the reverse cDNA confirmed that *cds9*, *trbM*, and *taxB* are, indeed, part of the *pilX* operon (Fig. 4B).

The 120-bp region upstream of the ATG start codon of *cds9*, named  $P_{pixR}$  was cloned upstream of a promoterless *lacZ* gene. The  $\beta$ -galactosidase activity was measured with and without ectopic expression of *pixR* in *E. coli* BW25113 in the absence of pHNSHP23. Without *pixR*, we detected a weak  $\beta$ -galactosidase activity for  $P_{pilX}$  that increased 130-fold upon *pixR* overexpression (Fig. 4C), confirming that PixR directly activates  $P_{pilX}$ .

To test whether PixR directly binds  $P_{pixR}$  we performed an electrophoretic mobility shift assay (EMSA) using the purified PixR protein. The 120-bp PCR-amplified  $P_{pilX}$  probe was incubated with increasing concentrations of purified PixR protein. The observed size shift of the fragment confirmed that PixR binds to  $P_{pilX}$  (Fig. 4D).

Together, these results demonstrate that PixR binds to the promoter region of the *pilX* operon and, by doing so, directly activates its transcription with very high efficiency *in vitro*.

**The ecological role of *pixR* in pHNSHP23.** Plasmid persistence in a bacterial community is usually associated with efficient acquisition and fitness benefits. To evaluate the ecological role of *pixR* in the persistence of pHNSHP23, we compared the ability of pHNSHP23 and its  $\Delta$ *pixR::cat* (Cm<sup>r</sup>) mutant to invade a plasmid-free population. The  $\Delta$ *pixR* plasmid failed to invade the plasmid-free population and was progressively lost after the first day (Fig. 5A). In contrast, pHNSHP23 gradually invaded the plasmid-free cells until the concentration of pHNSHP23-harboring cells equaled the concentration of plasmid-free cells (Fig. 5B). The population dynamics in competition cocultures were consistent with the observations in individual plasmid invasion assays (Fig. 5C). It is worthy of note that cell growth kinetics and pHNSHP23 stability remained unaffected by the  $\Delta$ *pixR* mutation over 10 days in pure culture (Fig. S1B and C). For this reason, and because the  $\Delta$ *pixR* plasmids were lost and failed to invade a population of plasmid-free cells, we hypothesized that the deletion of *pixR* induces a fitness cost. Hence,



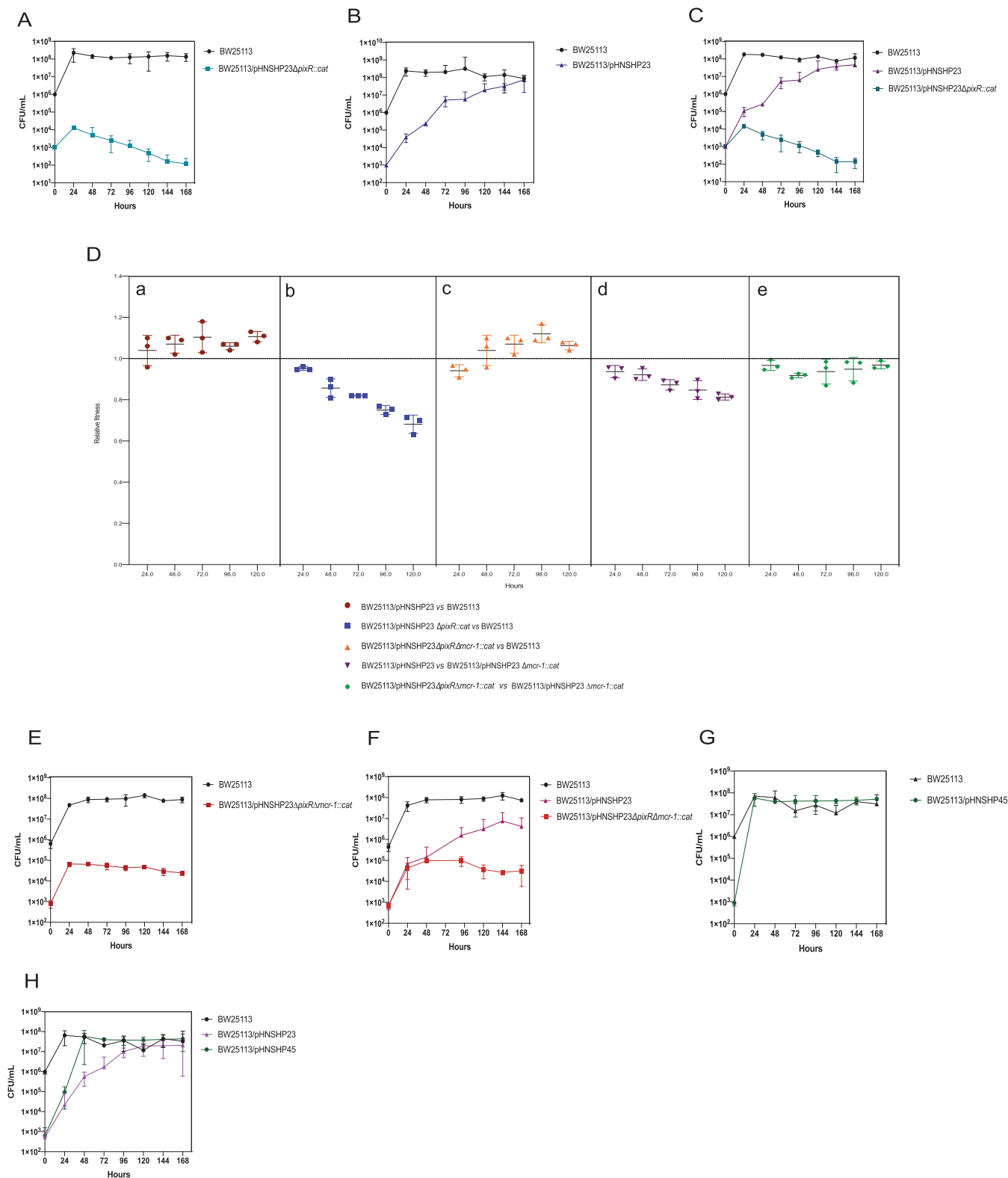


**FIG 5** Ecological role of *pixR* for plasmid pHNSHP23 invasion and persistence. *E. coli* BW25113/pHNSHP23Δ*pixR*::cat (A), BW25113/pHNSHP23 (B), BW25113/pHNSHP23Δ*pixR*Δ*mcr-1*::cat (E), and BW25113/pHNSHP45 (G) were mixed with a 1,000-fold excess of BW25113 without plasmid initially; BW25113/pHNSHP23Δ*pixR*::cat (C), BW25113/pHNSHP23Δ*pixR*Δ*mcr-1*::cat (F), and BW25113/pHNSHP45 (H) were cocultured with BW25113/pHNSHP23 and a 1,000-fold excess of BW25113 without plasmid initially. (D) *E. coli* BW25113/pHNSHP23, BW25113/pHNSHP23Δ*pixR*::cat, and BW25113/pHNSHP23Δ*pixR*Δ*mcr-1*::cat were competed with the reference strain BW25113 *in vitro*, separately. BW25113/pHNSHP23Δ*mcr-1* was competed with BW25113/pHNSHP23 *in vitro*. BW25113/pHNSHP23Δ*pixR*Δ*mcr-1*::cat was competed with BW25113/pHNSHP23Δ*mcr-1*::cat *in vitro*. All competitions assays were performed with three biological replicates.

Collectively, these results suggest that the increased rate of conjugation aids IncX4 plasmids in invading and persisting in bacterial populations. Because IncX4 and IncI2 plasmids are the main drivers of *mcr-1* spread, we compared their invasion capabilities using pHNSHP23 and pHNSHP45 as models, respectively. We found that pHNSHP45 invades cells at a much higher rate than pHNSHP23. pHNSHP45 had invaded most cells after 24 h under individual invasion conditions and after 48 h in competition cultures (Fig. 5G and H). In contrast, pHNSHP23 failed to overtake plasmid-free cells even after 5 days (Fig. 5B and H). The higher transfer rate reported for IncI2 plasmids ( $\sim 10^{-1}$  to  $10^{-3}$ ) than for IncX4 plasmids ( $\sim 10^{-2}$  to  $10^{-4}$ ) could explain these results (5).

**Comparative genomics of IncX plasmids.** We then searched the GenBank database for PixR protein homologues using blastp and found that 243 out of 272 IncX4 plasmids encode PixR (Table S1), while the other 29 IncX4 plasmids encode two types of PixR-like proteins (PixR-1 and PixR-2) sharing 46% identity with PixR of pHNSHP23 (Fig. S1). Of note, all *mcr-1*-positive IncX4 plasmids encode PixR (Table S1). Beyond the IncX4 family, a putative regulatory protein encoded by IncX7 plasmids p3 and pJARS35 from *Yersinia pestis* shares 54% identity with PixR. In addition, two PixR-like proteins encoded by two Col plasmids and other small untyped plasmids also share 44% and 49% identity with PixR. No other PixR-like proteins were identified in other IncX plasmids (Fig. S1).

Considering that *pixR* is a transfer activator specific to IncX4 and IncX7 plasmids, we compared the transfer genes of different IncX subgroups. We found that the conjugative transfer locus *taxB-pilX-taxCA* of the archetypical IncX2 plasmid R6K (GenBank accession no. [AJ006342](#)) shares >68% identity with the corresponding locus of the other representative IncX plasmids pOLA52 (IncX1a [[EU370913](#)]), R485 (IncX1b [[HE577112](#)]), pEC14\_35 (IncX3 [[JN935899](#)]), pBK31567 (IncX5 [[JX193302](#)]), and pCAV1043-58 (IncX8 [[CP011588](#)]), except for the entry exclusion gene *eex* of IncX1b plasmid R485. In contrast, the corresponding locus of plasmids pHNSHP23 (IncX4) and p3 (IncX7 [[CP009993](#)]), while exhibiting >70% identity with each other, share less than 25% identity with plasmids of the other IncX groups (Fig. 6). Furthermore, *eex*, found between *pilX5* and *pilX6* in most IncX subgroups, is located upstream of *pilX1* in pHNSHP23 and p3. Finally, *pixR* in pHNSHP23 and p3 is missing in other IncX subgroup plasmids where *actX* is found instead (Fig. 6 and Table S6). Pairwise sequence comparison showed no significant similarities between *actX* and *pixR*.

## DISCUSSION

IncX4 plasmids carrying *mcr-1* have been detected in over 41 countries and regions. Given the central role of conjugative plasmids in the global spread of antibiotic resistance, it has become imperative to understand the factors contributing to the dissemination of *mcr-1*-bearing IncX4 plasmids. In this study, we screened systematically for genes involved in the conjugative transfer of IncX4 plasmids. We identified a novel transfer activator, PixR, that contains the conserved C-terminal DNA-binding domain of LuxR proteins. We showed that PixR directly activates the expression of a set of core transfer genes by binding to the promoter of the transfer operon. Using HDTM, we identified 18 genes in pHNSHP23 that are essential for conjugative transfer. Thirteen of them were found to be upregulated upon overexpression of *pixR*, indicating that *pixR* is a potent and crucial activator of IncX4 conjugation. To the best of our knowledge, few studies have explored the regulation of the conjugative transfer of IncX plasmids. In IncX3 plasmids, the absence of a plasmid-encoded H-NS-like protein upregulates the expression of transfer genes through an uncharacterized pathway, causing a 2.5-fold increase in transfer frequency of IncX3 plasmids (33). Thus, PixR is the first transcriptional activator of transfer genes identified in IncX plasmids, which expands our knowledge of the conjugation of IncX plasmids. Like its homologue TraR, encoded by the Ti plasmid of *A. tumefaciens*, PixR belongs to the LuxR family of proteins. TraR requires the binding of 3-oxo-octanoyl-homoserine lactone (OC8HSL) to its N-terminal moiety to upregulate the expression of the T4SS-encoding *tral-trbCDEJKLFGHI* operon, leading to the activation of transfer (34–36). Our data seem to indicate that PixR lacks

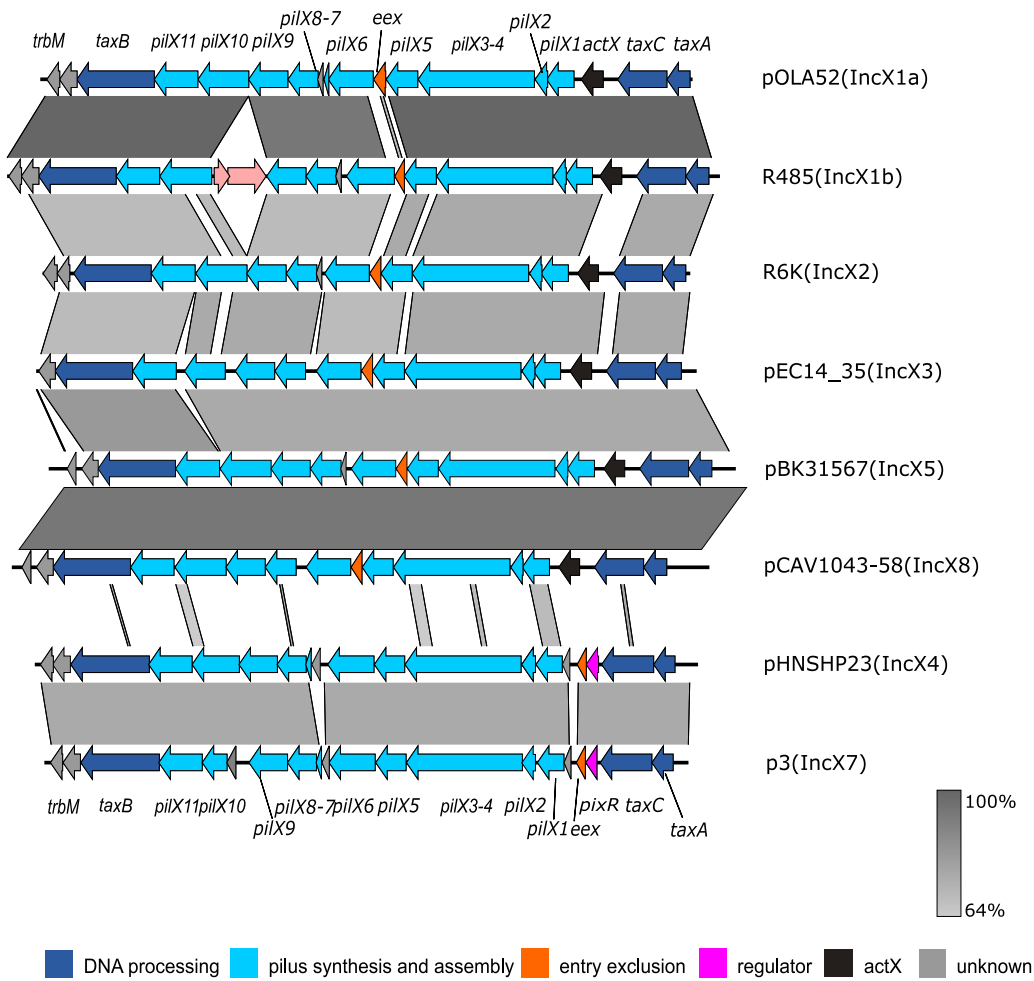


**FIG 6** Linear comparison of IncX plasmid transfer region. Genes are labeled in different colors based on their annotation. Shades of gray indicate percent sequence identity.

the ligand-binding domain. Further studies are needed to explore its activation mechanism. In particular, the signals that activate the expression of *pixR* are still unknown. The sequence divergence of IncX4 and IncX7 plasmid transfer regions with those of other IncX subgroups and the substitution of *actX* for *pixR* suggest that the PixR-based regulatory mechanism is specific to IncX4 and IncX7 plasmids. The genetic determinants that regulate the conjugal transfer of other IncX subgroups still need to be identified. The presence of *pixR* in Col or small untyped plasmids suggests a common regulatory mechanism in these plasmids and the possibility of coregulation if these plasmids coexist in the same host.

The conservation of *pixR* in the IncX4 plasmids suggests that this gene provides an evolutionary advantage for *mcr-1*-bearing IncX4 in nature. *pixR* increases the transfer capability of IncX4 plasmids, while a high rate of conjugation usually helps plasmids invade bacterial populations (20, 21, 37). Therefore, we investigated the role of *pixR* in the persistence and invasion of *mcr-1*-bearing IncX4 plasmids to better understand their prevalence. We found that pHNSHP23 lacking *pixR* inflicts a fitness cost to an *E. coli* host after 24 h of culture. The inactivation of *mcr-1* lessened this burden. These results demonstrate that efficient conjugation is sufficient to overcome the fitness cost of low-copy-number *mcr-1* carriage. The presence of *pixR* increases the transfer capability of IncX4 plasmids, minimalizing the fitness cost exerted by *mcr-1* carriage, resulting in the successful dissemination of *mcr-1*-bearing IncX4 plasmids. Through plasmid invasion assays, we found that pHNSHP23 lacking *pixR* loses its invasion capability and

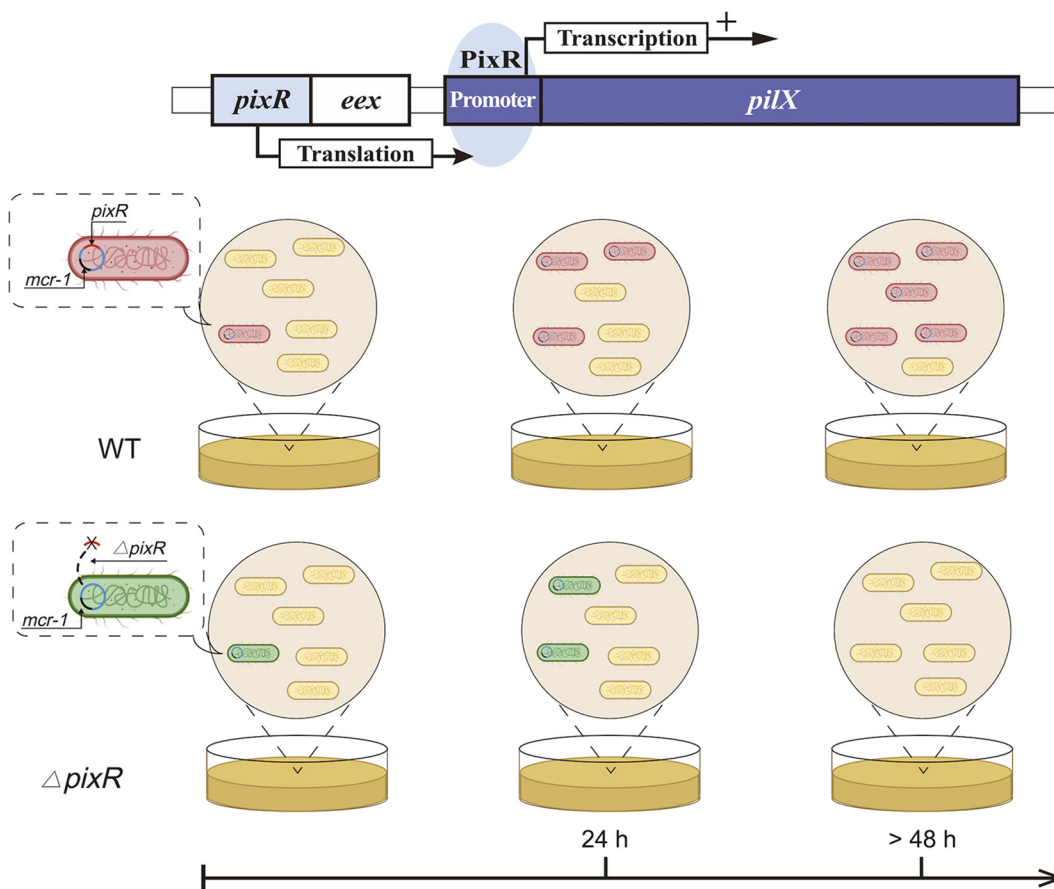


**FIG 7** PixR's key role in the persistence and invasion of *mcr-1*-bearing IncX4 plasmids. PixR enhances the conjugation efficiency of IncX4 plasmids by binding the promoter of a set of essential transfer genes to increase their expression. PixR has a strong effect on the persistence of *mcr-1*-bearing IncX4 plasmids in bacterial populations.

fails to establish stably in the cell population, suggesting that *pixR* is important for the survival of *mcr-1*-bearing IncX4 in a bacterial community (Fig. 7). Even though pHNSHP23 was able to invade a plasmid-free population, the rate of invasion was much lower than that of IncI2 plasmid pHNSHP45, which overtakes a plasmid-free population within 24 to 48 h. Such a difference likely results from a higher rate of transfer of IncI2 plasmids than of IncX4 plasmids (5), which could also explain the lower detection rate of IncX4 plasmids than of IncI2 plasmids after the withdrawal of colistin as a growth promoter in China (6). Overall, our data highlight that the efficient conjugation of plasmids plays an important role in the prevalence and persistence of *mcr-1*-bearing plasmids. Both strict control of low plasmid copy number and efficient conjugation contribute to the global prevalence of *mcr-1*-bearing plasmids (8).

A limited (1- to ~3-fold) change in *pilX3-4* and *pilX11* expression was observed between wild-type pHNSHP23 and its  $\Delta$ *pixR* mutant from RNA-seq and RT-qPCR data. Comparatively, a 3- to ~6-fold increase in *pixR*, *pilX3-4*, and *pilX11* expression was observed upon contact with *E. coli* C600. These data suggest that under nonmating conditions, PixR is either not active or sequestered. Alternatively, *pixR* expression is possibly repressed by another unknown factor in *E. coli* under laboratory conditions. However, *pixR* appears to be expressed under mating conditions, although the exact mechanism of activation remains unknown. This result is consistent with previous reports showing that repression of the conjugative transfer functions enhances the fitness of the bacterial host. Transfer genes are usually repressed, with only a few cells in the population expressing the conjugative machinery (34, 38, 39). A plausible hypothesis could be the transient elicitation of *pixR* expression or PixR activity in a small subset

of cells in the donor population upon contact with a potential recipient cell, such as a former donor cell having recently lost pHNSHP23 due to *mcr-1* carriage. *pixR* would then compensate the cost associated with *mcr-1* by enhancing conjugative transfer for a limited number of donor cells to maintain the balance of plasmid gain and loss. The slight increase that we observed at the population scale could very well be related to a subpopulation-specific activation. Future work will be conducted to confirm this hypothesis and unravel the complete regulatory mechanism of transfer activation in IncX4 plasmids.

In conclusion, we characterized an IncX4-specific regulatory mechanism that controls plasmid conjugation and showed that efficient conjugation is important to alleviate the fitness cost of *mcr-1* carriage and promote the persistence and invasion of *mcr-1*-bearing plasmids within a bacterial population. Given the significant role of high conjugation frequency of plasmids in the spread of antibiotic resistance genes, plasmid transfer inhibitors are noble approaches for solving the antibiotic resistance crisis. A deeper knowledge of the regulation of plasmid conjugation will provide potential targets for conjugation inhibition. Our data provide a new target to inhibit the dissemination of antibiotic resistance genes, especially *mcr-1*, mediated by IncX4 plasmids.

## MATERIALS AND METHODS

**Bacterial strains, plasmids and culture conditions, genetic constructions, bacterial conjugation experiments, and comparative sequence analyses.** The strains and plasmids used in this study are listed in Table S2. The primers used in this study are listed in Table S3. The details of culture conditions, genetic constructions, bacterial conjugation experiments and comparative sequence analyses are described in Text S1.

**Competition experiments *in vitro*.** The strains BW25113/pHNSHP23, BW25113/pHNSHP23Δ*pixR*::*cat*, and BW25113/pHNSHP23Δ*pixR*Δ*mcr-1*::*cat* were used to compete against BW25113, BW25113/pHNSHP23Δ*pixR*Δ*mcr-1*::*cat* was used to compete against BW25113/pHNSHP23Δ*mcr-1*::*cat*, and strain BW25113/pHNSHP23Δ*mcr-1*::*cat* was used to compete against BW25113/pHNSHP23. All competition assays were carried out in biological triplicates. The overnight cultures of the two competitors were mixed in equal volumes. Cultures were grown for 5 days with a 1:1,000 dilution into fresh LB broth every 24 h. At each 24-h time point, cultures were serially diluted and plated on LB agar plates containing colistin (Cl) or chloramphenicol (Cm). Considering that BW25113/pHNSHP23Δ*pixR*Δ*mcr-1*::*cat* and BW25113/pHNSHP23Δ*mcr-1*::*cat* could both be present on Cm plates, we distinguished these two strains by colony PCR with primers *pixRc*\_F/R. The following formula was used:

$$RF = \frac{\ln(N_{f,s1}/N_{i,s1})}{\ln(N_{f,s2}/N_{i,s2})}$$

where RF is the related fitness of strain S1 compared to strain S2 and  $N_{f,sx}$  and  $N_{i,sx}$  correspond to the CFU counts of strain *sx* at the observed time point and at the initial time point, respectively.

**Plasmid invasion assays.** Plasmid invasion assays were performed based on the protocol described previously, with some modifications (22). Briefly, overnight cultures of the recipient strain BW25113 were diluted 1:100 in LB medium and mixed with a 1:10,000 dilution of the overnight cultures of the donor strain (either BW25113/pHNSHP23, BW25113/pHNSHP45 BW25113/pHNSHP23Δ*pixR*::*cat*, or BW25113/pHNSHP23Δ*pixR*Δ*mcr-1*::*cat*). Cultures were grown in 50-mL tubes containing 2 mL LB broth at 37°C with slow rolling (80 rpm). Every 24 h, cultures were diluted 1:100 into fresh LB broth. Viable counts were gathered at 24, 48, 72, 96, 120, 144, and 168 h by plating serially diluted cultures on nonselective Cm- or Cl-containing LB agar. CFU counts for each type of plate were used to estimate the relative quantity of cells from the donor and recipient strains. For BW25113/pHNSHP23Δ*pixR*Δ*mcr-1*::*cat* and BW25113/pHNSHP23 Δ*pixR*::*cat*, we used the number of CFU counted on Cm plates. For BW25113/pHNSHP23, we used the number of CFU counted on Cl plates. Finally, for BW25113, we subtracted the CFU counted on Cl plates or Cm plates from the ones counted on nonselective plates. Competitive experiments were performed in a similar fashion by coinoculating three strains: either (i) BW25113, BW25113/pHNSHP23, and BW25113/pHNSHP23Δ*pixR*::*cat*, (ii) BW25113, BW25113/pHNSHP23, and BW25113/pHNSHP23Δ*pixR*Δ*mcr-1*::*cat*, or (iii) BW25113, BW25113/pHNSHP23, and BW25113/pHNSHP45. Counts for BW25113/pHNSHP23 were obtained by subtracting CFU counted on Cm plates from CFU counted on Cl plates. To distinguish between BW25113/pHNSHP23 and BW25113/pHNSHP45 (which would both grow on Cl plates), colonies were tested by PCR with primers IncI2-F/R and IncX4-F/R (Table S3).

**Cappable-seq, RNA-seq, HDTM, and reverse transcription and qPCR.** A thorough description of Cappable-seq, RNA-seq, and high-density transposon mutagenesis (HDTM), as well as reverse transcription and qPCR, is provided in Text S1.

**Protein purification, EMSA and β-galactosidase assay.** The details of protein purification, electrophoretic mobility shift assay (EMSA), and β-galactosidase assay are described in Text S1.

**Statistical analyses and figures.** Prism 9 (GraphPad Software) was used to generate graphics and perform statistical analyses. Figures were prepared with Inkscape 1.0.1 (<https://inkscape.org/>) and BioRender (<https://biorender.com/>).

**Data availability.** Complete data from aligned reads for HDTM, Cappable-seq, and RNA-seq experiments can be visualized using the UCSC genome browser at <http://bioinfo.ccs.usherbrooke.ca/pHNSHP23.html>.

Raw sequencing data were submitted to GenBank under BioProject accession number PRJNA759279 with the following BioSample accession numbers: for Cappable-seq assays, SRR15681005 to SRR15681011 and SRR15681020; for RNA-seq assays, SRR15681012 to SRR15681030 (except SRR15681020); and for HDTM assays, SRR15699958 to SRR15699960.

## SUPPLEMENTAL MATERIAL

Supplemental material is available online only.

**TEXT S1**, DOCX file, 0.05 MB.

**FIG S1**, DOCX file, 2.1 MB.

**FIG S2**, DOCX file, 2.9 MB.

**TABLE S1**, XLSX file, 0.03 MB.

**TABLE S2**, DOCX file, 0.03 MB.

**TABLE S3**, DOCX file, 0.02 MB.

**TABLE S4**, DOCX file, 0.01 MB.

**TABLE S5**, XLSX file, 0.1 MB.

**TABLE S6**, DOCX file, 0.02 MB.

## ACKNOWLEDGMENTS

This work was supported by the National Natural Science Foundation of China (grant no. 31830099 and 31625026), the Laboratory of Lingnan Modern Agriculture Project (NT2021006), the 111 Project (no. D20008), and the Innovation Team Project of Guangdong University (no. 2019KCXTD001).

V.B. was supported by a discovery grant (RGPIN-2016-04365) from the Natural Sciences and Engineering Research Council of Canada (NSERC) and a project grant (PJT-153071) from the Canadian Institutes of Health Research (CIHR). R.D. is the recipient of a Fonds de recherche du Québec-Nature et Technologies (FRQNT) doctoral fellowship.

J.-H.L., V.B., and L.Y. designed the study. L.Y., J.Y., and K.Y. performed experiments. L.Y., R.D., F.G., V.B., and J.-H.L. analyzed the data and prepared the figures. L.Y., J.-H.L., V.B., R.D., and F.G. drafted the manuscript. All authors reviewed, revised, and approved the final manuscript. Lingxian Yi and Romain Durand contributed equally to this work. Lingxian Yi is listed first because she was involved in most of the data analysis and experiments, except for bioinformatic analysis. Romain Durand is listed second because he was responsible for most of the bioinformatic analysis, including RNAseq and Chappableseq data analyses. He drafted the method and trained Lingxian Yi to perform library construction.

## REFERENCES

- World Health Organization. The ISSN register. <https://www.who.int/news-room/fact-sheets/detail/antibiotic-resistance>. Accessed 31 July 2020.
- Benz F, Huisman JS, Bakkeren E, Herter JA, Stadler T, Ackermann M, Diard M, Egli A, Hall AR, Hardt WD, Bonhoeffer S. 2021. Plasmid- and strain-specific factors drive variation in ESBL-plasmid spread in vitro and in vivo. *ISME J* 15:862–878. <https://doi.org/10.1038/s41396-020-00819-4>.
- Loftie-Eaton W, Yano H, Burleigh S, Simmons RS, Hughes JM, Rogers LM, Hunter SS, Settles ML, Forney LJ, Ponciano JM, Top EM. 2016. Evolutionary paths that expand plasmid host-range: implications for spread of antibiotic resistance. *Mol Biol Evol* 33:885–897. <https://doi.org/10.1093/molbev/msv339>.
- Taccconelli E, Carrara E, Savoldi A, Harbarth S, Mendelson M, Monnet DL, Pulcini C, Kahlmeter G, Kluytmans J, Carmeli Y, Ouellette M, Outtersson K, Patel J, Cavalieri M, Cox EM, Houchens CR, Grayson ML, Hansen P, Singh N, Theuretzbacher U, Magrini N, WHO Pathogens Priority List Working Group. 2018. Discovery, research, and development of new antibiotics: the WHO priority list of antibiotic-resistant bacteria and tuberculosis. *Lancet Infect Dis* 18: 318–327. [https://doi.org/10.1016/S1473-3099\(17\)30753-3](https://doi.org/10.1016/S1473-3099(17)30753-3).
- Liu Y-Y, Wang Y, Walsh TR, Yi L-X, Zhang R, Spencer J, Doi Y, Tian G, Dong B, Huang X, Yu L-F, Gu D, Ren H, Chen X, Lv L, He D, Zhou H, Liang Z, Liu J-H, Shen J. 2016. Emergence of plasmid-mediated colistin resistance mechanism MCR-1 in animals and human beings in China: a microbiological and molecular biological study. *Lancet Infect Dis* 16:161–168. [https://doi.org/10.1016/S1473-3099\(15\)00424-7](https://doi.org/10.1016/S1473-3099(15)00424-7).
- Liu YY, Zhou Q, He W, Lin Q, Yang J, Liu JH. 2020. mcr-1 and plasmid prevalence in *Escherichia coli* from livestock. *Lancet Infect Dis* 20:1126. [https://doi.org/10.1016/S1473-3099\(20\)30697-6](https://doi.org/10.1016/S1473-3099(20)30697-6).
- Wu R, Yi LX, Yu LF, Wang J, Liu Y, Chen X, Lv L, Yang J, Liu JH. 2018. Fitness advantage of mcr-1-bearing IncI2 and IncX4 plasmids in vitro. *Front Microbiol* 9:331. <https://doi.org/10.3389/fmicb.2018.00331>.
- Yang J, Wang HH, Lu Y, Yi LX, Deng Y, Lv L, Burrus V, Liu JH. 2021. A ProQ/FinO family protein involved in plasmid copy number control favours fitness of bacteria carrying mcr-1-bearing IncI2 plasmids. *Nucleic Acids Res* 49:3981–3996. <https://doi.org/10.1093/nar/gkab149>.
- Yi LX, Liu YY, Wu R, Liang ZS, Liu JH. 2017. Research progress on the plasmid-mediated colistin resistance gene mcr-1. *Yi Chuan* 39:110–126. <https://doi.org/10.16288/j.yczz.16-331>.
- Doumith M, Godbole G, Ashton P, Larkin L, Dallman T, Day M, Day M, Muller-Pebody B, Ellington MJ, de Pinna E, Johnson AP, Hopkins KL,

- Woodford N. 2016. Detection of the plasmid-mediated *mcr-1* gene conferring colistin resistance in human and food isolates of *Salmonella enterica* and *Escherichia coli* in England and Wales. *J Antimicrob Chemother* 71:2300–2305. <https://doi.org/10.1093/jac/dkw093>.
11. Mendes Oliveira VR, Paiva MC, Lima WG. 2019. Plasmid-mediated colistin resistance in Latin America and Caribbean: a systematic review. *Travel Med Infect Dis* 31:101459. <https://doi.org/10.1016/j.tmaid.2019.07.015>.
  12. Krutova M, Kalova A, Nycova E, Gelbicova T, Karpiskova R, Smelikova E, Nyc O, Drevinek P, Tkadlec J. 2021. The colonisation of Czech travellers and expatriates living in the Czech Republic by colistin-resistant Enterobacteriaceae and whole genome characterisation of *E. coli* isolates harbouring the *mcr-1* genes on a plasmid or chromosome: a cross-sectional study. *Travel Med Infect Dis* 39:101914. <https://doi.org/10.1016/j.tmaid.2020.101914>.
  13. Ma Z, Liu J, Chen L, Liu X, Xiong W, Liu JH, Zeng Z. 2021. Rapid increase in the IS26-mediated *cfr* gene in *E. coli* isolates with IncP and IncX4 plasmids and co-existing *cfr* and *mcr-1* genes in a swine farm. *Pathogens* 10:33. <https://doi.org/10.3390/pathogens10010033>.
  14. Espinal P, Miro E, Segura C, Gomez L, Plasencia V, Coll P, Navarro F. 2018. First description of blaNDM-7 carried on an IncX4 plasmid in *Escherichia coli* ST679 isolated in Spain. *Microb Drug Resist* 24:113–119. <https://doi.org/10.1089/mdr.2017.0039>.
  15. Bouma JE, Lenski RE. 1988. Evolution of a bacteria/plasmid association. *Nature* 335:351–352. <https://doi.org/10.1038/335351a0>.
  16. Baltus DA. 2013. Exploring the costs of horizontal gene transfer. *Trends Ecol Evol* 28:489–495. <https://doi.org/10.1016/j.tree.2013.04.002>.
  17. San Millan A, MacLean RC. 2017. Fitness costs of plasmids: a limit to plasmid transmission. *Microbiol Spectr* 5:MTBP-0016-2017. <https://doi.org/10.1128/microbiolspec.MTBP-0016-2017>.
  18. Dunn SJ, Connor C, McNally A. 2019. The evolution and transmission of multi-drug resistant *Escherichia coli* and *Klebsiella pneumoniae*: the complexity of clones and plasmids. *Curr Opin Microbiol* 51:51–56. <https://doi.org/10.1016/j.mib.2019.06.004>.
  19. Wyres KL, Holt KE. 2018. *Klebsiella pneumoniae* as a key trafficker of drug resistance genes from environmental to clinically important bacteria. *Curr Opin Microbiol* 45:131–139. <https://doi.org/10.1016/j.mib.2018.04.004>.
  20. Stewart FM, Levin BR. 1977. The population biology of bacterial plasmids: a priori conditions for the existence of conjugationally transmitted factors. *Genetics* 87:209–228. <https://doi.org/10.1093/genetics/87.2.209>.
  21. Miki T, Ueki M, Kawabata Z, Yamamura N. 2007. Long-term dynamics of catabolic plasmids introduced to a microbial community in a polluted environment: a mathematical model. *FEMS Microbiol Ecol* 62:211–221. <https://doi.org/10.1111/j.1574-6941.2007.00357.x>.
  22. Haft RJ, Mittler JE, Traxler B. 2009. Competition favours reduced cost of plasmids to host bacteria. *ISME J* 3:761–769. <https://doi.org/10.1038/ismej.2009.22>.
  23. Sun J, Fang LX, Wu Z, Deng H, Yang RS, Li XP, Li SM, Liao XP, Feng Y, Liu YH. 2017. Genetic analysis of the IncX4 plasmids: implications for a unique pattern in the *mcr-1* acquisition. *Sci Rep* 7:424. <https://doi.org/10.1038/s41598-017-00095-x>.
  24. Partridge SR, Ellem JA, Tetu SG, Zong Z, Paulsen IT, Iredell JR. 2011. Complete sequence of pJIE143, a *pir*-type plasmid carrying ISEcp1-blaCTX-M-15 from an *Escherichia coli* ST131 isolate. *Antimicrob Agents Chemother* 55:5933–5935. <https://doi.org/10.1128/AAC.00639-11>.
  25. Nunez B, Avila P, de la Cruz F. 1997. Genes involved in conjugative DNA processing of plasmid R6K. *Mol Microbiol* 24:1157–1168. <https://doi.org/10.1046/j.1365-2958.1997.4111778.x>.
  26. Ilangovan A, Connery S, Waksman G. 2015. Structural biology of the Gram-negative bacterial conjugation systems. *Trends Microbiol* 23:301–310. <https://doi.org/10.1016/j.tim.2015.02.012>.
  27. Gibert M, Juarez A, Zechner EL, Madrid C, Balsalobre C. 2014. TrhR, TrhY and HtdA, a novel regulatory circuit that modulates conjugation of the IncHI plasmids. *Mol Microbiol* 94:1146–1161. <https://doi.org/10.1111/mmi.12823>.
  28. Frost LS, Koraimann G. 2010. Regulation of bacterial conjugation: balancing opportunity with adversity. *Future Microbiol* 5:1057–1071. <https://doi.org/10.2217/fmb.10.70>.
  29. Carraro N, Matteau D, Luo P, Rodrigue S, Burrus V. 2014. The master activator of IncA/C conjugative plasmids stimulates genomic islands and multidrug resistance dissemination. *PLoS Genet* 10:e1004714. <https://doi.org/10.1371/journal.pgen.1004714>.
  30. Hancock SJ, Phan MD, Luo Z, Lo AW, Peters KM, Nhu NTK, Forde BM, Whitfield J, Yang J, Strugnell RA, Paterson DL, Walsh TR, Kobe B, Beatson SA, Schembri MA. 2020. Comprehensive analysis of IncC plasmid conjugation identifies a crucial role for the transcriptional regulator AcaB. *Nat Microbiol* 5:1340–1348. <https://doi.org/10.1038/s41564-020-0775-0>.
  31. Chen J, Xie J. 2011. Role and regulation of bacterial LuxR-like regulators. *J Cell Biochem* 112:2694–2702. <https://doi.org/10.1002/jcb.23219>.
  32. Ong CL, Beatson SA, McEwan AG, Schembri MA. 2009. Conjugative plasmid transfer and adhesion dynamics in an *Escherichia coli* biofilm. *Appl Environ Microbiol* 75:6783–6791. <https://doi.org/10.1128/AEM.00974-09>.
  33. Liu B, Shui L, Zhou K, Jiang Y, Li X, Guan J, Li Q, Zhuo C. 2020. Impact of plasmid-encoded H-NS-like protein on blaNDM-1-bearing IncX3 plasmid in *Escherichia coli*. *J Infect Dis* 221:S229–S236. <https://doi.org/10.1093/infdis/jiz2567>.
  34. McAnulla C, Edwards A, Sanchez-Contreras M, Sawers RG, Downie JA. 2007. Quorum-sensing-regulated transcriptional initiation of plasmid transfer and replication genes in *Rhizobium leguminosarum biovar viciae*. *Microbiology (Reading)* 153:2074–2082. <https://doi.org/10.1099/mic.0.2007/007153-0>.
  35. Li PL, Everhart DM, Farrand SK. 1998. Genetic and sequence analysis of the pTiC58 trb locus, encoding a mating-pair formation system related to members of the type IV secretion family. *J Bacteriol* 180:6164–6172. <https://doi.org/10.1128/JB.180.23.6164-6172.1998>.
  36. Zhang L, Murphy PJ, Kerr A, Tate ME. 1993. Agrobacterium conjugation and gene regulation by N-acyl-L-homoserine lactones. *Nature* 362:446–448. <https://doi.org/10.1038/362446a0>.
  37. Dionisio F, Matic I, Radman M, Rodrigues OR, Taddei F. 2002. Plasmids spread very fast in heterogeneous bacterial communities. *Genetics* 162:1525–1532. <https://doi.org/10.1093/genetics/162.4.1525>.
  38. Fernandez-Lopez R, Del Campo I, Revilla C, Cuevas A, de la Cruz F. 2014. Negative feedback and transcriptional overshooting in a regulatory network for horizontal gene transfer. *PLoS Genet* 10:e1004711. <https://doi.org/10.1371/journal.pgen.1004711>.
  39. Kozłowicz BK, Shi K, Gu ZY, Ohlendorf DH, Earhart CA, Dunny GM. 2006. Molecular basis for control of conjugation by bacterial pheromone and inhibitor peptides. *Mol Microbiol* 62:958–969. <https://doi.org/10.1111/j.1365-2958.2006.05434.x>.